INSTITUTE OF PHYSICS PUBLISHING JOURNAL OF PHYSICS: CONDENSED MATTER

J. Phys.: Condens. Matter **19** (2007) 056007 (13pp) doi:10.1088/0953-8984/19/5/056007

Ab initio calculations of the hydrogen centres in CaF_2 and BaF_2

H Shi[1,3], **R I Eglitis**[2] **and G Borstel**[1]

[1] Fachbereich Physik, Universität Osnabrück, D-49069 Osnabrück, Germany
[2] Department of Material Science and Engineering, Sung Kyun Kwan University, Suwon, Kyunggido, 440-746, Korea

E-mail: hshi@uos.de

Received 8 September 2006, in final form 24 November 2006
Published 15 January 2007
Online at stacks.iop.org/JPhysCM/19/056007

Abstract

As an extension of our previous studies dealing with bulk and surface F centres in CaF_2 and BaF_2, we have calculated the hydrogen impurity in CaF_2 and BaF_2 crystals. Our calculated absorption energy for the hydrogen impurity in CaF_2 (8.17 eV) is close to the experimental result (7.65 eV). The band and electronic structures are calculated and compared to the F centre case. We found that insertion of the hydrogen impurity in the bulk does not cause significant relaxation of the neighbouring atoms, but the relaxation of the atoms around the hydrogen impurity at surfaces is not negligible any more. We also observe a strengthening of the surface hydrogen centre and metal chemical bond with respect to the bulk.

(Some figures in this article are in colour only in the electronic version)

1. Introduction

Contemporary knowledge of defects in solids has helped to create a field of technology, namely *defect engineering*, which is aimed at manipulating the nature and concentration of defects in a material so as to tune its properties in a desired manner or to generate new behaviour. Alkaline earth fluorides could have important technical applications if one could avoid or, at least, control the defect formation. Therefore, it is important to understand the nature of defects in alkaline earth fluorides. It has always been a dream of materials researchers to design a new material completely on paper, optimizing the composition and processing steps in order to achieve the properties required for a given application. In principle, this should be possible, because all the properties of a material are determined by the constituent atoms and the basic laws of quantum mechanics. This approach of using only knowledge of the composition of a material to predict properties is referred to as a first-principles or *ab initio* calculation. The predictive

[3] Author to whom any correspondence should be addressed.

power of first-principles quantum electronic structure calculations due to increased speed of computers and recent developments of new and powerful computational methods allows for the rational design on paper of new materials for technology applications. One good example is the recent prediction of the average battery voltage for a series of cathode materials from first-principles calculations by Ceder [1, 2]. Currently available lithium-ion batteries are operating mainly in the 4 V regime. Based on calculations by Eglitis and Borstel [3], it was shown that a $Li_2Co_1Mn_3O_8$ cathode material can lead to a lithium-ion battery operating at the 5 V regime.

Considering the high technological importance of CaF_2 and BaF_2, it is not surprising that, during the last few years, it has been the subject of many experimental and theoretical studies [4–19]. Certain aspects of this research recently gained strong interest in the context of the use of CaF_2 as an optical material for the deep ultraviolet (DUV) and vacuum ultraviolet (VUV) spectral regions. BaF_2 is the fastest luminescent material that has been found to date [20]. Recently, BaF_2 has also been found to exhibit superionic conductivity by dissolving appropriate impurities into the lattice or by introducing an interface that causes the redistribution of ions in the space charge region, and is therefore considered as a candidate material for high-temperature batteries, fuel cells, chemical filters and sensors [21].

Many alkali halides provide an attractive medium for colour centre research because of the ease with which they can be grown in reasonably pure single-crystal form and because they may be coloured by ionizing radiation. Two kinds of intrinsic colour centres have been observed in CaF_2 and BaF_2 by electron spin-resonance techniques. One is the V_k, or self-trapped hole, whose resonance has been reported by Hayes and Twidell [22] in x-rayed CaF_2 at liquid-nitrogen temperatures (LNT) and by Nepomnyashchikh *et al* [23] in x-rayed BaF_2 at 77 K. The other is the F centre, an electron trapped in an anion vacancy, whose resonance has been found by Nepomnyashchikh *et al* [23] and Arends [24] in additively coloured BaF_2 and CaF_2 crystals, respectively, and calculated theoretically by Shi *et al* [4, 5].

Coloration effects in alkaline earth fluorides are strongly influenced by impurities. Hydrogen and oxygen impurities are two kinds of important point defects which affect the behaviour of alkaline earth fluorides under ionizing radiations, because they act as hole traps and under certain circumstances introduce anion vacancies into the crystals. Hydrogen-doped crystals colour quickly under x-irradiation at room temperature because of rapid generation of F-aggregate centres [25]. Using infrared methods, it was shown by Elliott *et al* [26] that crystals treated in this way contain hydrogen dissolved as H^- ions in fluorine sites (H_s^- centres) and concentrations of H_s^- approaching 10^{20} cm^{-3} are readily achieved. X-irradiation at room temperature also produced hydrogen atoms that are stable in interstitial sites (H_i^0 centres) [27]. It was shown by Bessent *et al* [28, 29], using electron paramagnetic resonance (EPR) methods, that x-irradiation at 77 K produced hydrogen atoms in fluorine sites (H_s^0 centres) and that the H_s^0 centres are converted to H_i^0 centres on warming to room temperature.

In this paper, we performed *ab initio* calculations to determine the electronic structure and atomic geometry of the H_s^- and H_i^0 centres in CaF_2 and BaF_2 crystals.

2. Method of calculations

The calculations for the hydrogen centres in CaF_2 and BaF_2 crystals were performed using the hybrid exchange–correlation functional (B3PW) involving a hybrid of non-local Fock exact exchange, local density approximation (LDA) exchange and Beckes gradient corrected exchange functional [30], combined with the nonlocal gradient corrected correlation potential by Perdew and Wang [31–33]. It is well known that the Hartree–Fock (HF) method considerably overestimates the optical band gap and density functional theory (DFT) underestimates it, but the hybrid B3PW method allows us to achieve good results. The hybrid

B3PW functional has been proved to yield remarkably accurate electronic and geometrical structures for CaF_2 and BaF_2 crystals [4, 5], as well as for ABO_3 perovskites [34–36]. Additionally, according to our previous studies dealing with F and *oxygen* centres, the B3PW method also gives reliable band gaps for these defect systems.

To perform the first-principles DFT-B3PW calculations, we used the CRYSTAL2003 computer code [37]. This code employs Gaussian-type functions (GTF) localized at atoms as the basis for an expansion of the crystalline orbitals. Features of the code, which are most important for this study, are its ability to calculate the electronic structure of materials within both Hartree–Fock and Kohn–Sham (KS) Hamiltonians. Another advantage of the code is its treatment of purely two-dimensional slabs, without artificial periodicity in the direction perpendicular to the surface, commonly employed in most other surface calculations [38, 39].

In order to employ the LCAO-GTF (linear combination of atomic orbitals) method, it is desirable to have optimized basis sets (BS). Such BS optimization for $BaTiO_3$ perovskite was developed and discussed in [35, 36]. In the present paper, we used this new BS for the Ba atom. For the Ca and F atoms, we used the same basis sets as in our previous study, dealing with the CaF_2 electronic structure and F centres therein [4]. For the H atom, we used the basis set developed by Dovesi *et al* [40]. The reciprocal space integration was performed by sampling the Brillouin zone of the unit cell with the $8 \times 8 \times 8$ Pack–Monkhorst net [41].

In the present paper, we used a *periodic supercell* model of the hydrogen centre. For the H_s^- centres, we started with a 81-atom supercell with one of the fluorine ions substituted by a H^- ion. For the H_i^0 case, we inserted one hydrogen atom into an atomic interstitial site of the 81-atom supercell. The 81-atom supercell is a primitive face-centred cubic (fcc) unit cell which is extended three times along all three translation vectors. After the hydrogen atom substitutes or is inserted, the atomic configuration of the surrounding atoms is re-optimized via a search of the total energy minimum as a function of the atomic displacements from the regular lattice sites.

In our previous paper dealing with F centres in CaF_2 [4], we carefully investigated the effect of the supercell size on various defect properties. We found that the F centre formation energy in CaF_2 converges at 7.87 eV for a supercell containing 48 atoms. The width of the defect band is then only 0.07 eV. Because of the more localized electron of the hydrogen centre, the interaction between the periodically repeated defects will be less than in the F-centre case. Therefore, we believe that a 81-atom supercell is sufficient in the present case.

At this point, we should address the question of the stability of the hydrogen impurities. As mentioned above, experimental works have clearly shown that hydrogen impurities can be trapped in several local minima of the energy hypersurface and thus show metastability. Typical activation barriers for conversion from the fluorine site to the interstitial site are of the order of 0.37 eV for CaF_2 and 0.33 eV for BaF_2 [25]. Therefore, the quantum effect should be negligible and, within the Born–Oppenheimer approximation, it should be a sound procedure to treat the hydrogen as a classical particle. This is in accordance with other recent theoretical work, i.e. on interstitial hydrogen in $PbTiO_3$ [42].

3. Calculated results for the H_s^- centres in CaF_2 and BaF_2 bulk

Figure 1 shows the geometry relaxations of the atoms surrounding the H_s^- centre in CaF_2 and BaF_2; see also table 1. For the CaF_2 H_s^--centre case, the conclusion is that, unlike the repulsive displacements of the four nearest Ca atoms surrounding the F centre in CaF_2 crystal [4], the Ca atoms are slightly displaced toward the H_s^- centre. The six second-nearest F atoms also move toward the hydrogen. For the BaF_2 H_s^--centre system, the four nearest Ba atoms are displaced

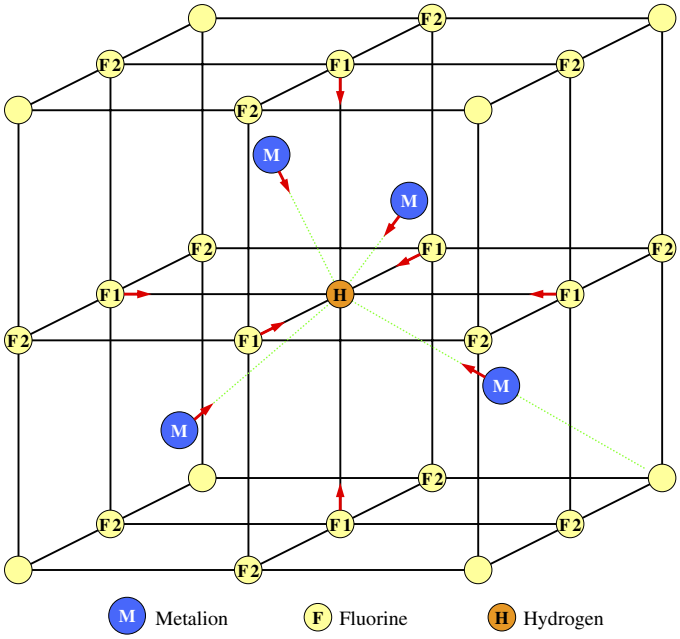

Figure 1. A view of the H_s^--centre nearest-neighbour geometry with the indication of relaxation shifts. According to the symmetries of the atoms, different labels are defined in circles.

Table 1. Atomic relaxations of 10 atoms surrounding a H_s^- centre in CaF_2 and BaF_2 81-atom supercells (as a percentage of the lattice constants, $a_0 = 5.50$ Å for CaF_2, $a_0 = 6.26$ Å for BaF_2). Positive signs indicate outward movements from the H_s^- centre.

Atoms	Number	CaF_2 D (a_0%)	BaF_2 D (a_0%)
M	4	−0.04	+0.09
F1	6	−0.13	−0.08

outward from the hydrogen and therefore have opposite directions with respect to the CaF_2 case. According to our calculations, we find that all these relaxations are very small. This phenomenon can be explained by looking at the effective charges.

To characterize the chemical bonding and covalency effects, we used a standard Mulliken population analysis for the effective atomic charges Q and other local properties of electronic structure (bond orders, atomic covalencies and full valencies) as described, for example, in [43, 44]. The charge density map for the H_s^- centre in CaF_2 bulk is shown in figure 2. The H_s^- centre for the BaF_2 crystal has a similar charge density map. Table 2 presents the effective charges of the H_s^- centre and the surrounding atoms. The analysis shows that the effective charge of the hydrogen ion in CaF_2 and BaF_2 is close to the F ion charge in CaF_2 and BaF_2 perfect crystals. These calculated results explain the negligible relaxations of the atoms surrounding the H_s^- centre. According to our calculations, although the F ion charges in CaF_2 are quite different from those in BaF_2, the effective charges (-0.895 e) of the H_s^- centre are almost the same in both materials. For the CaF_2 case, the charge difference (0.007 e) of the H_s^- centre is almost localized on the four nearest Ca atoms. For the BaF_2 crystal, around -0.016 e and -0.006 e from the H_s^- are localized on the four nearest Ba atoms and the six second-nearest-neighbour fluorine atoms, respectively.

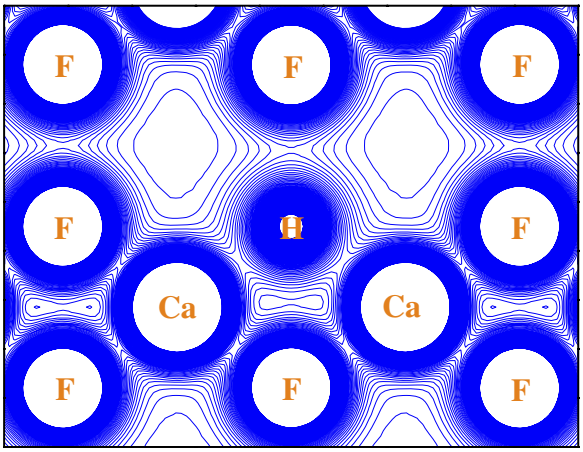

Figure 2. Charge density map of a CaF_2 crystal with the periodic H_s^- centre from the (1 1 0) side view. Isodensity curves are drawn from $0e$ bohr^{-3} to $0.2e$ bohr^{-3} with an increment of $0.002e$ bohr^{-3}.

Table 2. Effective charges ($Q(e)$) of the H_s^- centre and surrounding atoms in the CaF_2 and BaF_2 bulk. $\Delta Q(e)$ is the charge difference between the defective and perfect CaF_2 /BaF_2 crystal. (For the CaF_2 bulk, Ca: $+1.803\ e$, F: $-0.902\ e$. For the BaF_2 bulk, Ba: $+1.845e$, F: $-0.923e$.)

		CaF_2		BaF_2	
Atoms	Number	$Q(e)$	$\Delta Q(e)$	$Q(e)$	$\Delta Q(e)$
H	1	-0.895	$+0.007$	-0.895	$+0.028$
M	4	$+1.801$	-0.002	$+1.841$	-0.004
F1	6	-0.902	0	-0.924	-0.001
F2	12	-0.901	$+0.001$	-0.923	0

Next, we calculated the band structure of the H_s^- centre in CaF_2 and BaF_2 bulks. The defect–defect coupling due to the periodically repeated defects in our supercell model is negligible for the 81-atom supercell, since the widths of the defect bands are only 0.004 eV for the CaF_2 case and 0.0005 eV for the BaF_2 crystal. It is well known that only the highest occupied one-electron level has a strict physical meaning in exact DFT, which is merely a formalism for the electronic ground state [45]. Thus it is an approximation only to determine optical absorption energies as a difference of one-electron energies. In the present case some justification can be drawn from the fact that our calculated band gap is reasonable and close to the experimental value. The H_s^- defect band at the Γ point is located 2.75 eV (CaF_2) and 3.07 eV (BaF_2) above the top of the valence band (VB) (see figure 3). This suggests a possible mechanism for the optical absorption. The experimentally observable optical absorption could be due to an electron transfer from the H_s^--centre ground state to the conduction band (CB) bottom. The corresponding calculated values for CaF_2 and BaF_2 are 8.17 and 8.27 eV, respectively. Experimentally, the transition energy of the H_s^- centre in CaF_2 is 7.65 eV, and our calculated result is in some agreement with the experiment [46]. For the BaF_2 case, this experimental value is 6.00 eV [46], and our calculation overestimates it by 2.27 eV.

In comparison with previous studies dealing with F centres in CaF_2 and BaF_2, we found that the H_s^- bands are located not so high above the top of the VB as for the F-centre cases. The corresponding value of the F centre in the CaF_2 bulk is 6.75 eV, much larger than for the H_s^-

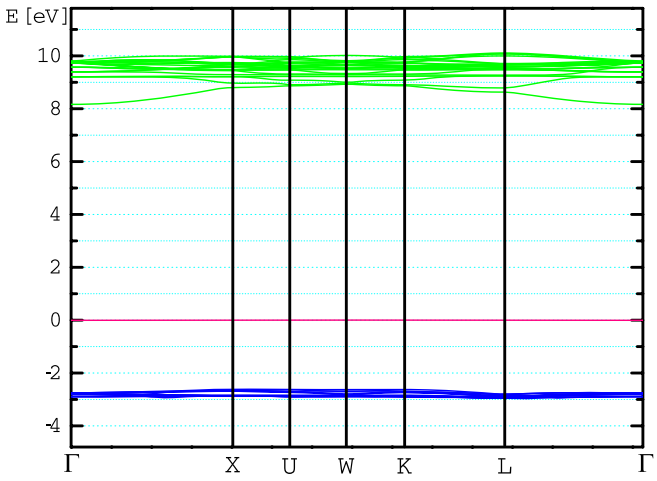

Figure 3. Calculated band structure for the 81-atom supercell modelling the H_s^- centre in CaF_2.

Table 3. Direct optical gaps (eV) ($\Gamma \rightarrow \Gamma$) of the H_s^- centre in the CaF_2 and BaF_2 bulk.

	CaF_2	BaF_2
$H_s^- \rightarrow$ CB	8.17	8.27
VB $\rightarrow H_s^-$	2.75	3.07

case (2.75 eV) (see table 3). For BaF_2, the F-centre band lies 7.01 eV above the VB top, but the H_s^- band is located only 3.01 eV above the VB top. We suggest that this phenomenon is due to the localization difference of the effective charge between the H_s^- centre and the F centre. The effective charge of the F centre in CaF_2 is $-0.752\ e$ and the H_s^-'s charge is $-0.895\ e$; this means that the H_s^- centre is more localized. A similar effect was also observed by us also for the oxygen-vacancy dipoles in CaF_2 [47].

The results of our calculations for the total and partial density of states (DOS) of the H_s^- centre show that the H_s^- s orbitals make the most contributions to the H_s^- band. The F p orbitals form the upper VB and the H_s^- defect level is primarily composed of hydrogen s orbitals, whereas the CB bottom consists mainly of metal ion d orbitals.

4. Calculated results for the H_i^0 centres in CaF_2 and BaF_2 bulk

We also investigated the H_i^0 centre, which is a hydrogen atom occupying an interstitial site (see figure 4). The analysis of the effective charges shows that the H_i^0-centre charge has a very small and negative value (see table 4). This charge arises mainly from the eight nearest fluorine ions. As we can see from table 4, the charge change of the nearest fluorine ions is $+0.014\ e$ for CaF_2 and $+0.009\ e$ for BaF_2. Bond population analysis shows that the bond populations between the hydrogen impurity atom and the nearest fluorine ions ($-26\ me$ for CaF_2 and $-2\ me$ for BaF_2) are close to the F–F bond populations in the perfect crystal ($-22\ me$ for CaF_2 and $-2\ me$ for BaF_2, respectively).

The relaxation of the atoms surrounding the H_i^0 centre is shown in figure 4. The conclusion is that the repulsions of the eight nearest F^- ions and the six second-nearest-neighbour metal ions from the H_i^0 centre for CaF_2 and BaF_2 are rather small (see table 5). These small outward

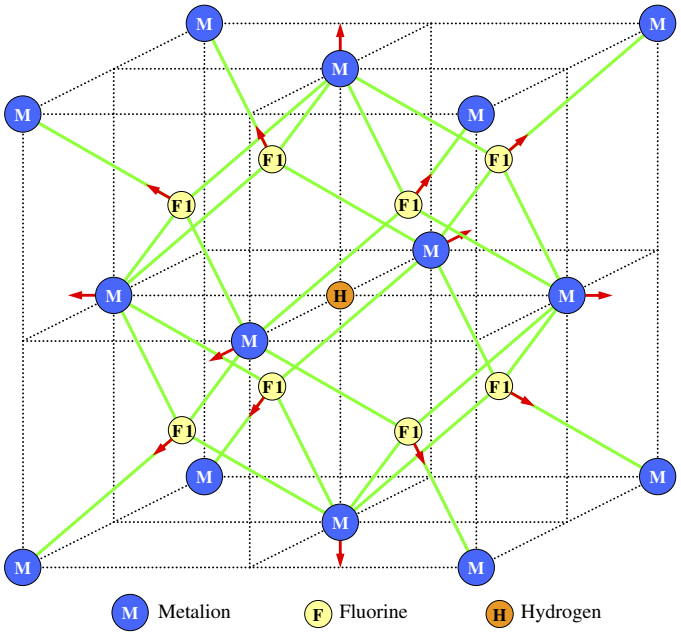

Figure 4. A view of the H_i^0-centre nearest-neighbour geometry with an indication of relaxation shifts.

Table 4. Effective charges ($Q(e)$) of the H_i^0 centre and surrounding atoms in the CaF_2 and BaF_2 bulk. $\Delta Q(e)$ is the charge difference between the defective and perfect CaF_2/BaF_2 crystal.

		CaF_2		BaF_2	
Atoms	Number	$Q(e)$	$\Delta Q(e)$	$Q(e)$	$\Delta Q(e)$
H	1	−0.097	—	−0.061	—
F	8	−0.888	+0.014	−0.914	+0.009
M	6	+1.801	−0.002	+1.844	−0.001

Table 5. Atomic relaxations of the atoms surrounding a H_i^0 centre in CaF_2 and BaF_2. Positive signs indicate the outward movements from the H_i^0 centre.

Atoms	Number	CaF_2 D (a_0%)	BaF_2 D (a_0%)
F1	8	+0.36	+0.17
M	6	+0.08	<+0.01

displacements of atoms surrounding the H_i^0 centre can be explained by the fact that the H_i^0 charge is close to zero.

To investigate the optical properties of H_i^0 centres in CaF_2 and BaF_2, we calculated the band structure of periodically repeated H_i^0 centre in our supercell model (see figure 5). The inserted hydrogen atom has only one electron, so there is an unpaired electron in each supercell. The presence of an unpaired electron is also revealed by the band structure of the defective system, given in figure 5. The bound unpaired electron level lies in the band gap; the corresponding unoccupied level appears in the β-spin structure, again in the gap, but at positive energies. Unlike unpolarized band structure curves whose states can be occupied by two electrons, only

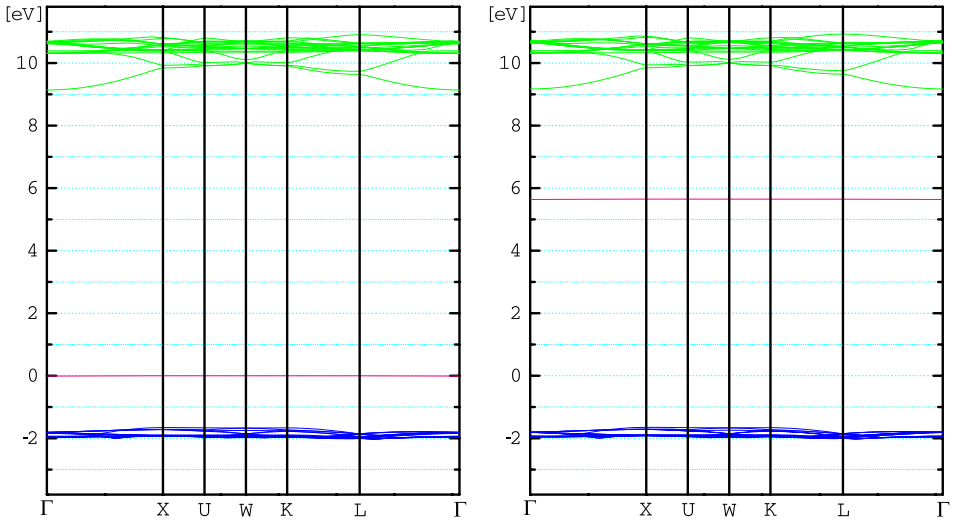

Figure 5. Calculated band structure for the 82-atom supercell modelling the H_i^0 centre in CaF_2. α (left) and β (right) denote the up- and down-spin states, respectively.

Table 6. Direct optical gaps (eV) ($\Gamma \rightarrow \Gamma$) of the H_i^0 centre in the CaF_2 and BaF_2 bulk.

	CaF_2		BaF_2	
Optical gaps	α	β	α	β
$H_i^0 \rightarrow$ CB	9.15	3.54	10.52	4.54
VB $\rightarrow H_i^0$	1.80	7.44	0.81	6.81

one electron occupies one state in figure 5. Following the previous discussion dealing with the H_s^- centre, we can now suggest a possible mechanism for the optical absorption of H_i^0-centre systems. In the ground state, the defect band is occupied in the α-spin system and unoccupied in the β-spin system (see figure 5). The optical absorption corresponds to an electron transition from the H_i^0-centre ground state to the CB. Because of the selection rules, an electron transition from the α occupied band to the β unoccupied band is forbidden. Our calculated optical gap between the α band and the CB is 9.15 and 10.52 eV for the CaF_2 and BaF_2 cases, respectively (see table 6). These values are larger than for the H_s^- case. Unfortunately, we did not find any experimental data for the H_i^0-centre optical absorption in literature.

The calculated total and partial density of states (DOS) of the H_i^0 centre in CaF_2 bulk are displayed in figure 6. The results of our calculations show, as in the H_s^- case, that the hydrogen s orbitals make the most contributions to the defect bands.

Due to the presence of an unpaired electron and the interaction between the unpaired spin and the spin of neighbouring nuclei, a hyperfine structure of the EPR spectra can be detected. The isotropic hyperfine interaction is caused by the non-zero probability of an electron being in the position of a given nucleus. The anisotropic contribution is due to the presence of higher-order poles, and it is indicative of the deformation of the electronic density with respect to the spherical distribution. Usually, the experimental hyperfine coupling data are reported in terms of the isotropic a and anisotropic b hyperfine coupling constants. For each nucleus N, they are expressed (in MHz) as [48]

$$a = \frac{2\mu_0}{3h} g\beta_e g_N \beta_n \rho^{\alpha-\beta}(0) \tag{1}$$

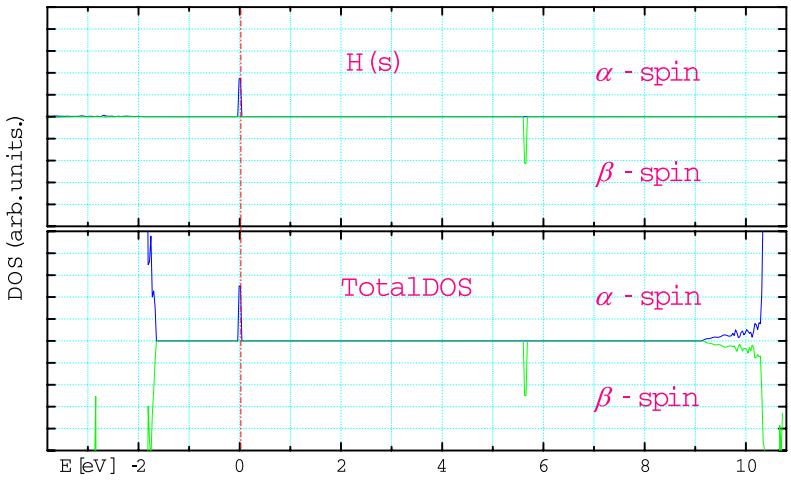

Figure 6. Total and projected density of states (DOS) for the H_i^0 centre in CaF_2 bulk. α and β denote the up- and down-spin states, respectively.

Table 7. Observed and calculated isotropic hyperfine constants a and anisotropic hyperfine constants b (MHz) for the H_i^0 centre in CaF_2 and BaF_2.

	CaF_2		BaF_2	
Hyperfine constant	Our results	Expt [27]	Our results	Expt [29]
a	99.5	104	38.6	41
b	35.2	34.93	20.9	21

$$b = \frac{\mu_0}{4\pi h} g\beta_e g_N \beta_n \left[T_{11} - \frac{1}{2}(T_{22} + T_{33}) \right] \tag{2}$$

where the spin density $\rho^{\alpha-\beta}$ at N, the elements of the hyperfine coupling tensor **T**, and the electron g factor are the only terms that depend on the electronic structure of the system. All other multiplicative factors in (1) and (2) are tabulated constants [48, 49] (h is the Planck constant, β_e and β_n the electronic and nuclear magnetons, μ_0 the permeability of the vacuum, and g_N the nuclear g factor). **T** is a tensor of rank 2, which is obtained as the field gradient of the spin density at N. Our calculated hydrogen and fluorine hyperfine parameters are compared with experiment in table 7 and are in a good agreement with experiment.

5. Surface H_s^- centres in CaF_2 and BaF_2

As an extension of our study dealing with H_s^- centres in CaF_2 and BaF_2 bulk, we investigated the H_s^- centre placed at the (111) surface, which is the most stable one among the (100), (110) and (111) terminated surfaces for CaF_2 and BaF_2 [4, 5]. In the present work, we performed our surface H_s^- centre calculations for a slab containing four layers. Each layer consists of three sublayers, containing nine atoms. Therefore, the supercell used in our calculations contains 108 atoms.

The relaxations of the atoms near the (111) surface are presented in table 8. The hydrogen ion at the surface moves outward by 1.02% of a_0 for CaF_2 and by 0.81% of a_0 for BaF_2. Otherwise, the six neighbouring F atoms at the same upper sublayer move inward. The

Table 8. Atomic relaxation of CaF_2 or BaF_2 slab containing a H_s^- centre located at the (111) surface (as a percentage of the lattice constant). Positive signs correspond to outward atomic displacements (toward the vacuum). The directions of atomic displacements in the XY-plane are indicated in figure 7.

		CaF_2		BaF_2	
Atoms	Number	XY	Z	XY	Z
H_s^-	1	—	+1.02	—	+0.81
F1	6	0.16	−0.59	0.25	−0.48
M (Ca/Ba)	3	0.12	−0.35	0.17	+0.55
F2	3	0.32	−0.52	0.51	−0.02

Table 9. The effective charges ($Q(e)$) of the surface H_s^- centre and surrounding atoms. $\Delta Q(e)$ is the charge difference between the defective slab and perfect CaF_2/BaF_2 bulk.

		CaF_2		BaF_2	
Atoms	Number	$Q(e)$	$\Delta Q(e)$	$Q(e)$	$\Delta Q(e)$
H_s^-	1	−0.877	+0.025	−0.894	+0.029
F1	6	−0.891	+0.011	−0.918	+0.005
M (Ca/Ba)	3	+1.794	−0.009	+1.834	−0.011
F2	3	−0.907	−0.005	−0.924	−0.001

relaxations of the three neighbouring metal ions at the middle sublayer of the surface layer, moving inward for CaF_2 and outward for BaF_2, are in qualitative agreement with our previous studies about the perfect (111) slabs for CaF_2 [4] and BaF_2 [5]. The H_s^-–M (metal ion) distance increases by 0.62% of a_0 for CaF_2 and by 0.15% of a_0 for BaF_2 with respect to the corresponding value of bulk H_s^- case. In comparison with the bulk case, we can conclude that the atoms surrounding the H_s^- centre show a stronger repulsion to the hydrogen ion located at the surface.

With respect to the electronic structure of the surface H_s^- centre, the effective charge analysis shows that the electronic density around it is slightly more delocalized than in the bulk. Table 9 presents the effective charge values of the surface H_s^- centre and surrounding atoms. The effective charge of the H_s^- centre is $-0.877\ e$, $0.018\ e$ less than for the bulk H_s^- centre in CaF_2 (see table 2). Otherwise, the BaF_2 surface H_s^- charge value is $-0.894\ e$, only $0.001\ e$ less than in the bulk. The charges of the nearest metal ions of the surface H_s^- centre ($+1.794\ e$ for CaF_2 and $+1.834\ e$ for BaF_2) are reduced by $0.007\ e$ and $0.007\ e$ in comparison with the charges of the relevant Ca ions ($+1.801\ e$) and Ba ions ($+1.841\ e$). Bond populations between the surface H_s^- centre and the nearest metal ions were also calculated. The major effect observed here is a strengthening of the surface H_s^- and M chemical bond. The surface H_s^-–Ca bond population is $+6\ me$ and larger than the corresponding value in the bulk by $18\ me$. For the BaF_2 case, there is a similar, but weaker strengthening effect of the H_s^-–Ba bond. The surface H_s^-–Ba bond population is $-30\ me$, which is larger than the relevant value in bulk by $6\ me$. This similar, but much stronger, effect, strengthening the Ti–O chemical bond near the surface, was also observed earlier for $SrTiO_3$ [34, 50].

The band structure of the surface H_s^- centre for CaF_2 is shown in figure 8. Similar results hold for BaF_2. The defect energy band is located 2.87 eV (0.12 eV higher than in the bulk H_s^--centre case) for CaF_2 and 2.86 eV (0.21 eV lower than in the bulk H_s^--centre case) for BaF_2 above the VB top and is separated from the CB bottom by 7.91 and 7.94 eV, respectively (see table 10). Because of the surface effect, according to our calculations, this gap is smaller

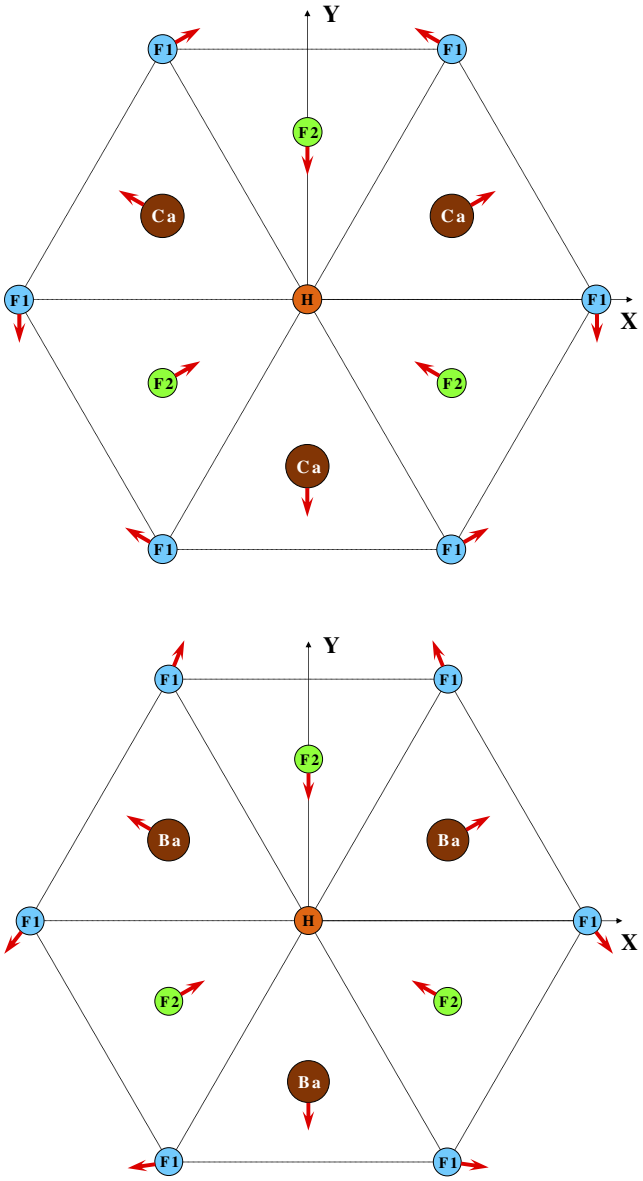

Figure 7. Top view of the surface H_s^--centre nearest-neighbour geometry with indication of the atomic displacement directions. F1 indicates the fluorine atoms located at the upper sublayer, and F2 the fluorine atoms located at the lower sublayer.

than the corresponding value in the bulk H_s^--centre case (8.17 eV) by 0.26 eV for CaF_2. For BaF_2, this gap is reduced by 0.33 eV with respect to the value of the bulk H_s^- centre (8.27 eV). The negligible dispersion effect of the defect band for a 108-atom supercell means that the defect–defect interaction is practically eliminated, thus approaching the desired isolated single H_s^--centre limit.

Further analysis of the layer-resolved DOS on an expanded energy scale shows the existence of an electronic surface state near the top of the VB. It is found that the DOS of

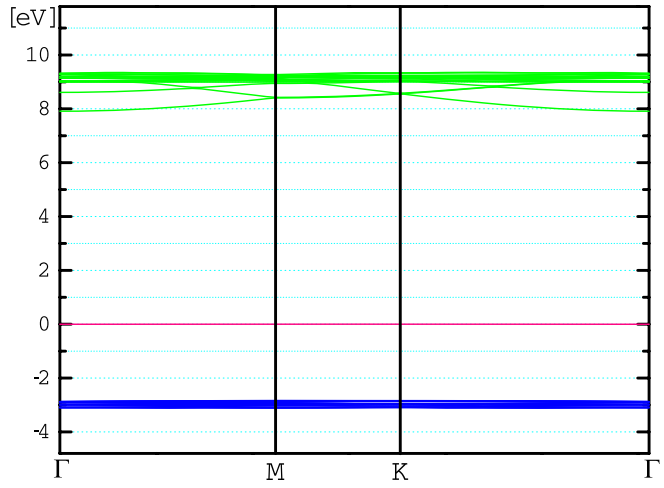

Figure 8. Calculated band structure for the 108-atom supercell modelling the H_s^- centre in CaF_2 (111) slab.

Table 10. Direct optical gaps (eV) ($\Gamma \rightarrow \Gamma$) of the (111) surface H_s^- centre in CaF_2 and BaF_2.

	CaF_2	BaF_2
$H_s^- \rightarrow$ CB	7.91	7.94
VB $\rightarrow H_s^-$	2.87	2.86

the p orbitals of the surface F ions moves towards higher energies and in this way splits off the bulk continuum. This mechanism is in fact the main reason for the narrowing of the gap at the (111) surface and it happens on both ideal and defective surfaces.

6. Conclusions

Our calculated optical absorption energy for hydrogen impurities (H_s^- centres) in CaF_2 (8.17 eV) is close to the experimental result of 7.65 eV, but is overestimated for the BaF_2 crystal. We found, that the defect band induced by hydrogen impurities in CaF_2 and BaF_2 is much closer to the VB top as it was for the F centres in CaF_2 and BaF_2. The hydrogen impurity bands in CaF_2 and BaF_2 crystals are located 2.75 and 3.07 eV, respectively, above the VB.

Our calculations show that the relaxation of the atoms around the hydrogen impurity in CaF_2 and BaF_2 bulk is very small, but the relaxation of surrounding atoms is no longer negligible for a hydrogen impurity located at CaF_2 and BaF_2 surfaces.

We also observed strengthening of the surface H_s^- and M (metal ion) chemical bond. The surface H_s^-–Ca bond population is $+6\ me$ and larger than the corresponding value in bulk by 18 me. A similar effect, strengthening of the metal–oxygen bond populations near the surfaces, was also observed by us earlier for ABO_3 provskites [34, 36, 50].

References

[1] Ceder G 1998 *Science* **280** 1099
[2] Ceder G, Chiang Y-M, Sadoway D R, Aydinol M K, Jang Y-I and Huan B 1998 *Nature* **392** 694
[3] Eglitis R I and Borstel G 2005 *Phys. Status Solidi* a **202** R13

[4] Shi H, Eglitis R I and Borstel G 2005 *Phys. Rev.* B **72** 045109
[5] Shi H, Eglitis R I and Borstel G 2006 *J. Phys.: Condens. Matter* **18** 8367
[6] Schmalzl K, Strauch D and Schober H 2003 *Phys. Rev.* B **68** 144301
[7] de Leeuw N H and Cooper T G 2003 *J. Mater. Chem.* **13** 93
[8] de Leeuw N H, Purton J A, Parker S C, Watson G W and Kresse G 2000 *Surf. Sci.* **452** 9
[9] Verstraete M and Gonze X 2003 *Phys. Rev.* B **68** 195123
[10] Rubloff G W 1972 *Phys. Rev.* B **5** 662
[11] Barth J, Johnson R L, Cardona M, Fuchs D and Bradshaw A M 1990 *Phys. Rev.* B **41** R3291
[12] Gan F, Xu Y N, Huang M Z, Ching W Y and Harrison J G 1992 *Phys. Rev.* B **45** 8248
[13] Ching W Y, Gan F and Huang M Z 1995 *Phys. Rev.* B **52** 1596
[14] Catti M, Dovesi R, Pavese A and Saunders V R 1991 *J. Phys.: Condens. Matter* **3** 4151
[15] Foster A S, Barth C, Shluger A L, Neiminen R M and Reichling M 2002 *Phys. Rev.* B **66** 235417
[16] Jockisch A, Schröder U, Wette F W and Kress W 1993 *J. Phys.: Condens. Matter* **5** 5401
[17] Puchin V E, Puchina A V, Huisinga M and Reichling M 2001 *J. Phys.: Condens. Matter* **13** 2081
[18] Merawa M, Lunell M, Orlando R, Gelize-Duvignau M and Dovesi R 2003 *Chem. Phys. Lett.* **368** 7
[19] Puchina A V, Puchin V E, Kotomin E A and Reichling M 1998 *Solid State Commun.* **106** 285
[20] Kawano K *et al* 1999 *Phys. Rev.* B **60** 11984
[21] Sata N, Eberman K, Eberl K and Maier J 2000 *Nature* **408** 946
[22] Hayes W and Twidell J W 1962 *Proc. Phys. Soc. Lond.* **79** 1295
[23] Nepomnyashchikh I, Radzabov E A, Egranov A V, Ivasheckin V F and Istomin A S 2002 *Radiat. Effects Defects Solids* **157** 715
[24] Arends J 1964 *Phys. Status Solidi* **7** 805
[25] Hayes W 1974 *Crystals with the Fluorite Structure* (Oxford: Clarendon)
[26] Elliott R J, Hayes W, Jones G D, Macdonald H F and Sennett C T 1965 *Proc. R. Soc.* A **289** 1
[27] Hall J L and Schumacher R T 1962 *Phys. Rev.* **127** 1892
[28] Bessent R G, Hayes W and Hodby J W 1967 *Proc. R. Soc.* A **297** 376
[29] Bessent R G, Hayes W, Hodby J W and Smith P H S 1969 *Proc. R. Soc.* A **309** 69
[30] Becke A D 1993 *J. Chem. Phys.* **98** 5648
[31] Perdew J P and Wang Y 1986 *Phys. Rev.* B **33** 8800
[32] Perdew J P and Wang Y 1989 *Phys. Rev.* B **40** 3399
[33] Perdew J P and Wang Y 1992 *Phys. Rev.* B **45** 13244
[34] Heifets E, Eglitis R I, Kotomin E A, Maier J and Borstel G 2001 *Phys. Rev.* B **64** 235417
[35] Piskunov S, Heifets E, Eglitis R I and Borstel G 2004 *Comput. Mater. Sci.* **29** 165
[36] Eglitis R I, Piskunov S, Heifets E, Kotomin E A and Borstel G 2004 *Ceram. Int.* **30** 1989
[37] Saunders V R, Dovesi R, Roetti C, Causa M, Harrison N M, Orlando R and Zicovich-Wilson C M 2003 *CRYSTAL-2003 User Manual* (Italy: University of Torino)
[38] Padilla J and Vanderbilt D 1998 *Surf. Sci* **418** 64
[39] Cheng C, Kunc K and Lee M H 2000 *Phys. Rev.* B **62** 10409
[40] Dovesi R *et al* 1984 *Phys. Rev.* B **29** 3591
[41] Monkhorst H J and Pack J D 1976 *Phys. Rev.* B **13** 5188
[42] Park C H and Chadi D J 2000 *Phys. Rev. Lett.* **84** 4717
[43] Catlow C R A and Stoneham A M 1983 *J. Phys. C: Solid State Phys.* **16** 4321
[44] Bochiccio R C and Reale H F 1993 *J. Phys. B: At. Mol. Opt. Phys.* **26** 4871
[45] Jones R O and Guunarsson O 1989 *Rev. Mod. Phys.* **61** 689
[46] Beaumont J H, Gee J V and Hayes W 1970 *J. Phys. C: Solid State Phys.* **3** L152
[47] Shi H, Eglitis R I and Borstel G 2006 *Comput. Mater. Sci.* at press
[48] Weil J A, Bolton J R and Wertz J E 1994 *Electron Paramagnetic Resonance* (New York: Wiley)
[49] Lide D (ed) 1991 *Handbook of Chemistry and Physics* 72nd edn (Boston, MA: CRC Press)
[50] Heifets E, Goddard W A III, Kotomin E A, Eglitis R I and Borstel G 2004 *Phys. Rev.* B **69** 035408